Spectrochimica Acta Part A: Molecular and Biomolecular Spectroscopy 119 (2014) 63–75

Contents lists available at SciVerse ScienceDirect

Spectrochimica Acta Part A: Molecular and Biomolecular Spectroscopy

journal homepage: www.elsevier.com/locate/saa

One- and two-photon absorption of fluorescein dianion in water: A study using S-QM/MM methodology and ZINDO method

D.L. Silva [a], R.C. Barreto [a,b], E.G. Lacerda Jr. [a], K. Coutinho [a], S. Canuto [a,*]

[a] Instituto de Física, Universidade de São Paulo, CP 66318, 05314-970 São Paulo, SP, Brazil
[b] Departamento de Física, Universidade Tecnológica Federal do Paraná, 80230-901 Curitiba, PR, Brazil

HIGHLIGHTS

- Theoretical study of the 1PA and 2PA spectra of fluorescein dianion in explicit water environment.
- The unusual blue shift of the lowest-energy $\pi \rightarrow \pi^*$ transition of FSD is properly described.
- The INDO/CI calculations provide a better description of the $\pi \rightarrow \pi^*$ transition of FSD than the TD-DFT.
- Solvent effects do not considerably change the 2PA cross-section of FSD along the entire spectrum.
- The RE method is an interesting way to study the 2PA of solvated molecules in microscopic detail.

GRAPHICAL ABSTRACT

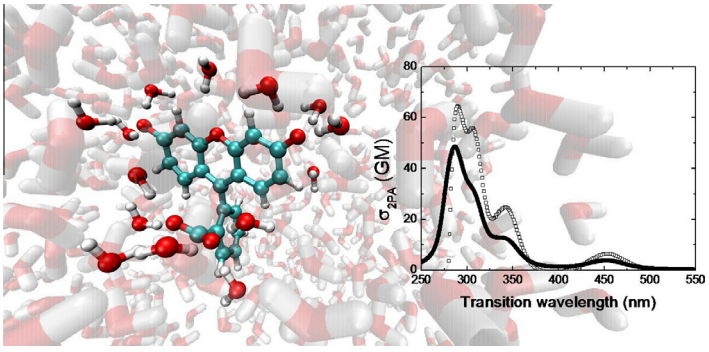

ARTICLE INFO

Article history:
Available online 15 April 2013

Keywords:
One-photon absorption
Two-photon absorption
Explicit/discrete solvent models
Sequential Quantum Mechanics/Molecular Dynamics methodology
Zerner's intermediate neglect of differential overlap (ZINDO) method
Sum-Over-States (SOS) model

ABSTRACT

One- and two-photon absorption (1PA and 2PA) of fluorescein dianion (FSD) in water were studied using a combined and sequential Quantum Mechanics/Molecular Dynamics methodology. Different sets of 250 statistically relevant (uncorrelated) configurations composed by the solute and several solvent molecules were sampled from the classical simulation. On these configurations, the electronic properties were calculated *a posteriori* using the Zerner's intermediate neglect of differential overlap (ZINDO) method. The linear and nonlinear absorption of FSD in water were calculated using discrete and explicit solvent models. In the largest case, the relevant configurations are composed by FSD and 47 explicit water molecules embedded in the electrostatic field of all remaining water molecules. Both INDO/CIS and INDO/CISD calculations were performed to study the absorption processes of FSD and the Sum-Over-States (SOS) model was used to describe the 2PA process. A semi-classical method for spectrum simulations was employed to simulate the 1PA and 2PA cross-section spectra of FSD in water. For comparison purposes, in the case of the 2PA process two approaches, the "full expression" and "resonant expression" methods, were employed to simulate the nonlinear spectrum. The last method assumes resonant conditions and on the computation point of view it represents an interesting option to study the 2PA process. The INDO/CI calculations give a satisfactory description of the 1PA spectrum of FSD and properly describe the unusual blue-shift of its first $\pi \rightarrow \pi^*$ transition in water. In the case of 2PA, the introduction of doubly excited configuration interactions (INDO/CISD) has proven to be essential for an appropriate description of the process at the higher energy spectral region. It was observed that the solvent effects do not drastically change the cross-sections of both processes. The simulated 2PA cross-section spectrum provided by the "full expression" method presents a better definition of the bands which appear along the experimental spectrum than the one provided by the "resonant expression" method. However, both approaches provide similar description for the effect of the solvent environment on the 2PA process of FSD in water.

* Corresponding author. Tel.: +55 11 3091 6980.
E-mail address: canuto@if.usp.br (S. Canuto).

1386-1425/$ - see front matter © 2013 Elsevier B.V. All rights reserved.
http://dx.doi.org/10.1016/j.saa.2013.04.035

Introduction

The optical behavior of materials plays a major role in the technology of photonics [1,2]. To further advance the performance of optical devices and techniques, researchers have sought for materials with attractive linear and nonlinear optical properties, what comprises the absorption, refractive and emission behavior of the materials. In the last decades the nonlinear optical properties of the materials has attracted growing attention. In this case, the organic materials have emerged as an interesting class due to present high nonlinear optical properties and the possibility of easily alter their molecular structure to optimize the nonlinear response [3].

Due to its potential applicability, the two-photon absorption (2PA) is one of the nonlinear processes which has attracted more attention in the last decades [1,2]. The applications of such nonlinear process have been manifested in several important areas [4–15]. Its quadratic dependence on the excitation light intensity is responsible for the improvement brought by the 2PA process to the 3D optical storage [4,5], 3D fluorescence microscopy [6,11,14] and 3D microfabrication [15] areas, since it intrinsically offers a high spatial confinement of the excitation. The quadratic dependence is also responsible for the improvement brought to the optical limiting area [7,12]. On the other hand, in the 2PA process two photons are simultaneously absorbed by a material and, therefore, the excitation energy is given by the sum of the energy of the two photons absorbed. Due to this feature, the 2PA process is also employed, for instance, at up-conversion lasing and fluorescence microscopy areas [6,8,9,11,14]. Moreover, the main limitations of photodynamic therapy are the low penetration and high scattering in tissue of the light used in treatments. In this case, the 2PA allows to excite photosensitisers absorbing light in the tissue optical window, improving the penetration and reducing the scattering of the laser light [10,13].

What concerns the fluorescence microscopy area, fluorescein is a widely used probe in biosciences [16–21], mainly because of its high fluorescence quantum efficiency (0.18–0.93) [22]. The use of fluorescein in 1PA and 2PA fluorescence microscopy has been reported in several works [23–26]. It is today well-known that fluorescein exists in several well-defined prototropic states and charge forms. Varying the pH of the aqueous environment, its charge state and consequently its absorption and fluorescence spectra change in a well defined manner [27–29]. For intermediate acidic values of pH, between 3.8 and 6.1, fluorescein exists in two possible mono-ionic forms and above pH 6.1 the dianionic form of fluorescein (Fig. 1) prevails. As for neutral pH fluorescein exists in its dianionic form, most of the experimental and theoretical works on the spectroscopic properties of fluorescein have focused on the fluorescein dianion (FSD).

The 1PA and 2PA spectra of FSD have been determined and reported in some experimental works [29–33]. Some theoretical efforts have also been carried out to study the 1PA and 2PA of FSD, and other charge forms of fluorescein, in the last few years

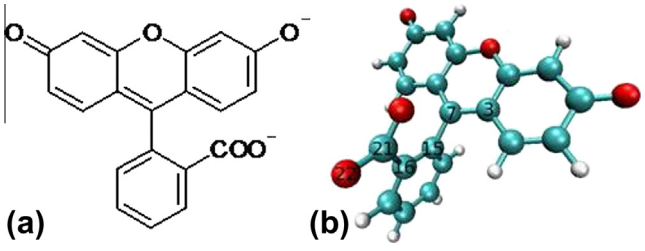

Fig. 1. (a) Molecular structure of fluorescein dianion (FSD). (b) Initial conformation (B3LYP/6-311++G(d,p), PCM – water) for classical simulation.

[34,35]. However, the effect of the solvent on the spectroscopic properties of fluorescein is still poorly understood. The majority of the theoretical studies concerning the linear and nonlinear absorption of FSD have been done for the isolated molecule or using a Polarizable Continuum Model (PCM) [36–38] for taking into account solvent effects. PCM has been widely used to attempt to describe solvent effects on the linear absorption of molecular systems and, more recently, to describe solvent effects on the nonlinear two-photon absorption [35,39–42]. This model usually gives a good description of the solvent effects for studies considering a polar solute and nonprotic solvents. However, the PCM is not able to include specific interactions such as hydrogen bonds for describing the solvent effects on the absorption processes, what is in principle an important aspect for studies considering the aqueous environment. Moreover, the important influence of the solvent on the 2PA process of organic molecules, in particular, has already been demonstrated by several experimental studies [43–46].

Among the most sophisticated strategies to study the absorption processes of molecular systems in solution are the Quantum Mechanics/Molecular Mechanics (QM/MM) methodologies [47–51]. These methodologies allow to include contributions coming from specific interactions between solute and solvent molecules, as well as the statistical information related to the thermodynamic conditions. Since the liquid has a huge amount of possible configurations, it is very important to properly describe the thermodynamic ensemble to study a solvated molecule. To generate the liquid structure, QM/MM methodologies use classical computer simulation, either Monte Carlo (MC) or Molecular Dynamics (MD). After that, quantum mechanical calculations are performed on sampled configurations.

Recently, we studied the spectral shift of the lowest and most intense 1PA transition of FSD in water [52]. The study was done under normal conditions of temperature and pressure using the sequential QM/MM (S-QM/MM) methodology [53–55] – combining MC simulation and INDO/CIS calculations. For the best of our knowledge, that was the first theoretical attempt to study FSD in aqueous environment in microscopic details. The S-QM/MM methodology offers the opportunity of drastically reducing the number of quantum mechanical calculations needed to obtain a statistically converged value of the spectroscopic properties of a given system. Unlike the traditional QM/MM methodologies, in the S-QM/MM methodology the quantum mechanical calculations are performed only on a set of statistically relevant (uncorrelated) configurations [53–55].

Both 1PA and 2PA spectra of FSD in water present interesting features which deserve attention and represent a challenge for theoretical methods [29,31,33]. The linear spectrum of FSD is mainly described by its lowest energy and most intense $\pi \rightarrow \pi^*$ transition which suffers an unusual blue-shift in water. The 2PA spectrum of FSD in water in turn is a structured spectrum where 3 bands can easily be distinguished. The widely use of FSD and its intriguing linear and nonlinear spectra were the main motivations to carry out this theoretical study.

In the present work we employed the S-QM/MM methodology [53–55] to study the one- and two-photon absorption of FSD in water under normal thermodynamic conditions. We decided to use MD simulation to include the effect of the FSD molecular conformation changes on the absorption spectra. INDO/CIS and INDO/CISD calculations were performed to study the 1PA and 2PA processes of FSD in water and the Sum-Over-States (SOSs) model [56] was used to describe the 2PA process. Several studies of the 2PA of molecular systems combining INDO/CI calculations and the SOS model have been carried out and reported in the last few years [57–61]. Studies of the 2PA process employing this strategy and considering the solvent environment in microscopic details are still lacking. In fact, to the best of your knowledge, the present

work is the first study conducted by combining such strategy and the S-QM/MM methodology to describe the 1PA and 2PA processes of a solvated molecule. However, it is important to mention that in the last years this issue has been addressed by studies employing different levels of quantum-chemical calculations and different QM/MM methodologies [62–64].

Adopting discrete and explicit solvent models, INDO/CI calculations were performed on the relevant configurations of the system and the results used to simulate the 1PA and 2PA cross-section spectra of FSD in aqueous environment. The use of a set of solvent models allowed to better understanding the origin of the solvent effects on the linear and nonlinear absorption of FSD in aqueous environment. A semi-classical method [65–67] for spectrum simulations was employed to simulate the absorption spectra. For comparison purposes, in the case of the 2PA process two approaches of the SOS model [56], labeled here as the "full expression" and "resonant expression" methods, were employed to simulate the nonlinear spectrum. As we discuss in Two-photon absorption section, the last method assumes two-photon resonant conditions and on the computation point of view it represents an interesting option to study the 2PA process.

Procedure

Classical simulation

The S-QM/MD methodology was adopted in this work. A MD simulation was performed under normal conditions (T = 25 °C, P = 1 atm) to generate the liquid structure that were submitted *a posteriori* to QM calculations. All MD simulations were done with TINKER molecular modeling package [68]. The initial configuration was generated from a previous MC simulation of FSD in water [52]. The thermalization stage was 200 ps and the equilibrium simulation was 5 ns, with a time step of 1 fs. One configuration was saved every 1 ps. The integrator algorithm was the velocity Verlet [69,70] and the algorithms used to control the temperature and pressure were the Berendsen thermostat and barostat respectively [71], with a coupling constant of 0.1 ps for temperature and 2.0 ps for pressure. A cubic box with periodic boundary conditions and a cut-off radius of 9.0 Å for non-bonded interactions were used. The long-range corrections were calculated for interactions and forces beyond the cut-off radius. The Coulomb term of the non-bonded interactions was corrected by particle mesh Ewald (PME) approach [72].

The simulated system consisted of one FSD and 1000 molecules of water. The intermolecular interaction was defined by a Lennard-Jones (LJ) plus Coulomb potentials. The intramolecular and LJ parameters of the optimized parameters for liquid simulation (OPLS) [73,74] was used for FSD and the SPC [75] potential for water. One important aspect prior to the MD simulation is the consideration of the electronic polarization of FSD due to the aqueous environment. To consider this polarization, the molecular geometry of FSD was obtained from a geometry optimization in water performing a PCM calculation [36–38]. The atomic charges of the Coulomb part of the potential of FSD were obtained using an electrostatic CHELPG mapping [76] in a PCM calculation using the optimized geometry of FSD. All the PCM calculations were performed using density functional theory (DFT) with the aid of the hybrid B3LYP functional [77,78] and the 6-311++G(d,p) basis set, as implemented in the Gaussian 03 package [79].

One-photon absorption

The 1PA of a given molecular system is related to the imaginary part of its linear polarizability, $\alpha(-\omega;\omega)$ [1,3], and can be quantized by the definition of the 1PA cross-section (σ_{1PA}). Employing the semi-classical approximation [80], the 1PA cross-section of a molecular system at the angular frequency ω of the incident laser light is defined as

$$\sigma_{1PA}(\omega) = \frac{4\pi\omega}{n^2 c} L^2 \mathrm{Im}[\langle\alpha(-\omega;\omega)\rangle] \tag{1}$$

where c is the speed of light, n is the refractive index of the medium and L is a local-field factor (equal to 1 for vacuum). In this study n and L are set to 1. $\langle\alpha(-\omega;\omega)\rangle$ is the orientational average of $\alpha(-\omega;\omega)$ and becomes the theoretical values provided by this equation comparable with experimental values measured in solution.

The components of the polarizability can be evaluated applying perturbation theory up to second-order in energy and the electric dipole approximation [56]. By considering the Taylor expansion of the energy with respect to an applied field, the Cartesian components of $\alpha(-\omega;\omega)$ are given by

$$\alpha_{ij}(-\omega;\omega) = \frac{1}{\hbar} \times \sum_{n\neq g}\left[\frac{\langle g|\mu_i|n\rangle\langle n|\mu_j|g\rangle}{(\omega_{gn}-\omega-i\Gamma_{gn}/2)} + \frac{\langle g|\mu_j|n\rangle\langle n|\mu_i|g\rangle}{(\omega_{gn}+\omega+i\Gamma_{gn}/2)}\right] \tag{2}$$

In Eq. (2), n denotes the nth electronic excited state and g the electronic ground state. $\langle g|\mu_j|n\rangle$ is the Cartesian component of the transition dipole moment from the ground state to the nth excited state along the molecular axis j. $\omega_{gn} = (E_n - E_g)/\hbar$ are the angular frequencies of the one-photon resonances. Γ_{gn} is the damping constant of the nth excited state adopted to treat the resonances. The sum is performed over the manifold of excited states of the unperturbed system. The orientational average of α is calculated via Eq. (3).

$$\langle\alpha\rangle = \frac{1}{3}\sum_{i=x,y,z}\alpha_{ii} \tag{3}$$

To study the 1PA of a molecular system, it is convenient to consider $\alpha(-\omega;\omega)$ for the angular frequencies of the one-photon resonances, i.e., $\omega = \omega_{gn}$. In this case, only contributions coming from the first term of Eq. (2) will resonate. If the damping constant Γ_{gn} is small compared to ω_{gn}, such contributions will dominate the complete summation and the second term can be neglected. Therefore, considering also the orientational average of $\alpha(-\omega;\omega)$, the linear absorption at the angular frequency ω of the incident laser light can thus be written as follows in

$$\sigma_{1PA}(\omega) = \frac{4\pi\omega}{3\hbar n^2 c} L^2 \sum_{n\neq g}\left[\sum_{i=x,y,z}|\langle g|\mu_i|n\rangle|^2 \frac{\Gamma_{gn}/2}{(\omega_{gn}-\omega)^2 + (\Gamma_{gn}/2)^2}\right] \tag{4}$$

From the spectroscopy point of view, in order to describe the 1PA of a system through a broad spectral region, it is necessary to consider the spectral line shape of the one-photon resonances. It is common to adopt a normalized Lorentzian function to this end. Here, it is possible to obtain it naturally, since Eq. (4) can be simply rewritten as

$$\sigma_{1PA}(\omega) = \frac{4\pi^2\omega}{3\hbar n^2 c} L^2 \sum_{n\neq g}|\mu_{gn}|^2 g(\omega_{gn}-\omega;\Gamma_{gn}) \tag{5}$$

where μ_{gn} is the transition dipole moment between the ground $|g\rangle$ and excited $|n\rangle$ electronic states and $g(\omega_{gn}-\omega;\Gamma_{gn})$ is the normalized Lorentzian function. Therefore, in addition to attribute a finite spectral line width (Γ_{gn}) for each excited state considered to study the linear spectrum of a given molecular system, the $g(\omega_{gn} - \omega;\Gamma_{gn})$ function also selects the resonant angular frequencies of the one-photon transitions between the ground and final excited states (ω_{gn}).

In this work the linear and nonlinear spectra of FSD in water were determined employing the semi-classical method [65–67].

In this method the absorption spectra are simulated by adopting the nuclear (solute-solvent) phase space distribution provided by the classical MD simulation. In the context of the S-QM/MM methodology, this is a set of uncorrelated configurations (MD snapshots) sampled from the liquid simulation process. As has been shown in a previous work [67], the simulated 1PA cross-section spectrum can be obtained by the average over the absorption behavior of the ensemble,

$$\sigma_{1PA}(\omega) = \frac{4\pi^2\omega}{3\hbar n^2 c} L^2 \sum_{n\neq g}^{N_{fs}} \left[\frac{1}{N_c} \sum_{k}^{N_c} |\mu_{gn}^k|^2 g(\omega_{gn}^k - \omega; \Gamma_{gn}) \right] \tag{6}$$

In Eq. (6), N_c is the number of uncorrelated configurations sampled and N_{fs} the number of final excited states considered to simulate the linear spectrum. The superscript k refers to the kth uncorrelated configuration sampled. The term in the brackets is the average intensity of a given 1PA transition of the system studied. In this approach, while Γ_{gn} in the $g(\omega_{gn}^k - \omega; \Gamma_{gn})$ function accounts for the homogeneous broadening of the resonance lines playing along the 1PA spectrum, the classical simulation intrinsically accounts for their inhomogeneous broadening. Therefore, this procedure provides a realistic picture of the absorptive behavior of a molecule in solvent environment through a broad spectral region.

Two-photon absorption

The 2PA process corresponds to the simultaneous absorption of two photons and is only promoted using high intensity laser light. The two-photon absorption of a given molecular system is quantized by the 2PA cross-section (σ_{2PA}) which in turn is proportional to the imaginary part of the second order hyperpolarizability, $\gamma(-\omega_\sigma; \omega_1, \omega_2, \omega_3)$ [1,3]. Employing the semi-classical approximation [80] and considering a degenerate 2PA process, the nonlinear absorption at the angular frequency ω of the incident laser light is defined as follows

$$\sigma_{2PA}(\omega) = \frac{8\pi^2\hbar\omega^2}{n^2c^2} L^4 \mathrm{Im}[\langle\gamma(-\omega;\omega,-\omega,\omega)\rangle] \tag{7}$$

where $\langle\gamma(-\omega;\omega,-\omega,\omega)\rangle$ is the orientational average of $\gamma(-\omega;\omega,-\omega,\omega)$ and becomes the theoretical values provided by this equation comparable with experimental values measured in solution.

The components of the second-order hyperpolarizability can be evaluated applying perturbation theory up to fourth-order in energy and the electric dipole approximation. The expression obtained in this way is usually called the Orr-Ward or Sum-Over-State (SOS) expression [56]. By considering the Taylor expansion of energy with respect to an applied field, the Cartesian components of $\gamma(-\omega_\sigma; \omega_1, \omega_2, \omega_3)$, in the most general form, are given by

$$\gamma_{ijkl}(-\omega_\sigma;\omega_1,\omega_2,\omega_3) = \frac{1}{6\hbar^3} P(j,k,l;\omega_1,\omega_2,\omega_3) \times \left[\begin{aligned} &\sum_{m\neq g}\sum_{n\neq g}\sum_{p\neq g} \frac{\langle g|\mu_i|m\rangle\langle m|\bar{\mu}_l|n\rangle\langle n|\bar{\mu}_k|p\rangle\langle p|\mu_j|g\rangle}{(\omega_{gm}-\omega_\sigma+i\Gamma_{gm}/2)(\omega_{gn}-\omega_1-\omega_2+i\Gamma_{gn}/2)(\omega_{gp}-\omega_1+i\Gamma_{gp}/2)} \\ &+\frac{\langle g|\mu_l|m\rangle\langle m|\bar{\mu}_i|n\rangle\langle n|\bar{\mu}_k|p\rangle\langle p|\mu_j|g\rangle}{(\omega_{gm}+\omega_3-i\Gamma_{gm}/2)(\omega_{gn}-\omega_1-\omega_2+i\Gamma_{gn}/2)(\omega_{gp}-\omega_1+i\Gamma_{gp}/2)} \\ &\frac{\langle g|\mu_j|m\rangle\langle m|\bar{\mu}_k|n\rangle\langle n|\bar{\mu}_i|p\rangle\langle p|\mu_l|g\rangle}{(\omega_{gm}+\omega_l-i\Gamma_{gm}/2)(\omega_{gn}+\omega_1+\omega_2-i\Gamma_{gn}/2)(\omega_{gp}-\omega_3+i\Gamma_{gp}/2)} \\ &\frac{\langle g|\mu_j|m\rangle\langle m|\bar{\mu}_k|n\rangle\langle n|\bar{\mu}_l|p\rangle\langle p|\mu_i|g\rangle}{(\omega_{gm}+\omega_l-i\Gamma_{gm}/2)(\omega_{gn}+\omega_1+\omega_2-i\Gamma_{gn}/2)(\omega_{gp}+\omega_\sigma-i\Gamma_{gp}/2)} \\ &-\sum_{m\neq g}\sum_{n\neq g}\frac{\langle g|\mu_l|m\rangle\langle m|\mu_i|g\rangle\langle g|\mu_k|n\rangle\langle n|\mu_j|g\rangle}{(\omega_{gm}-\omega_\sigma+i\Gamma_{gm}/2)(\omega_{gn}-\omega_3+i\Gamma_{gn}/2)(\omega_{gn}-\omega_1+i\Gamma_{gn}/2)} \\ &+\frac{\langle g|\mu_i|m\rangle\langle m|\mu_l|g\rangle\langle g|\mu_k|n\rangle\langle n|\mu_j|g\rangle}{(\omega_{gm}-\omega_3+i\Gamma_{gm}/2)(\omega_{gn}+\omega_2-i\Gamma_{gn}/2)(\omega_{gn}-\omega_1+i\Gamma_{gn}/2)} \\ &+\frac{\langle g|\mu_l|m\rangle\langle m|\mu_i|g\rangle\langle g|\mu_j|n\rangle\langle n|\mu_k|g\rangle}{(\omega_{gm}+\omega_\sigma-i\Gamma_{gm}/2)(\omega_{gm}+\omega_3-i\Gamma_{gn}/2)(\omega_{gn}+\omega_1-i\Gamma_{gn}/2)} \\ &+\frac{\langle g|\mu_l|m\rangle\langle m|\mu_i|g\rangle\langle g|\mu_j|n\rangle\langle n|\mu_k|g\rangle}{(\omega_{gm}+\omega_3-i\Gamma_{gm}/2)(\omega_{gn}-\omega_2+i\Gamma_{gn}/2)(\omega_{gn}+\omega_l-i\Gamma_{gn}/2)}) \end{aligned} \right] \tag{8}$$

In Eq. (8), ω_1, ω_2 and ω_3 are the angular frequencies of the perturbation radiation fields and $\omega_\sigma = \omega_1 + \omega_2 + \omega_3$ is the polarization response angular frequency. $P(j,k,l;\omega_1,\omega_2,\omega_3)$ is a permutation operator which permutes the Cartesian coordinates labels (j,k,l) of the molecule axis and simultaneously permutes the optical angular frequencies $(\omega_1,\omega_2,\omega_3)$. m, n and p denote electronic excited states and g the electronic ground state. $\langle g|\mu_j|m\rangle$ is the jth Cartesian component of the transition dipole moment from the ground state to the m excited state. $< m|\overline{\mu}_j|n > = < m|\mu_j|n > - \delta_{mn} < g|\mu_j|g >$ is the fluctuation of the jth Cartesian component of the dipole moment operator (μ_j). Γ_{gm} is the damping constant of the m excited state. The orientational average of γ is calculated via Eq. (9) [81,82].

$$\langle\gamma\rangle = \frac{1}{15}\sum_{i,j=x,y,z}(\gamma_{iijj}+\gamma_{ijij}+\gamma_{ijji}) \tag{9}$$

In this work, the 2PA cross-section spectrum of FSD in water is simulated employing the semi-classical method to simulate absorption spectra and adopting two different approaches. In both cases, the simulated nonlinear spectrum is the average over the absorption behavior of the ensemble of uncorrelated configurations provided by the classical MD simulation.

In the first approach, as long as the main interest here is to describe the nonlinear absorption, the Eq. (8) is simplified assuming that it is possible to neglect the non-resonant terms. In reciprocity to the 1PA process, it is expected that some terms dominate $\gamma(-\omega;\omega,-\omega,\omega)$ around two-photon resonant angular frequencies, $\omega = \omega_{gn}/2$. Analyzing Eq. (8) one can verify that only some contributions coming from the first two terms of the triple summation will be resonant. If the damping constant Γ_{gn} is small compared to ω_{gn}, such terms will dominate the complete summation and all the remaining terms can be neglected. Moreover, when the angular frequency of the incident light is still low enough in comparison to the first one-photon resonant angular frequency of the system, one can adopt a null value for the damping constants of the intermediate states (Γ_{gm} and Γ_{gp}) on Eq. (8) without qualitative and quantitative losses. In this condition, the Cartesian components of $\gamma(-\omega;\omega,-\omega,\omega)$ can be written in a simpler and more convenient way as

$$\begin{aligned} &\gamma_{ijkl}^{res}(-\omega_\sigma;\omega_1,\omega_2,\omega_3) \\ &= \frac{1}{6\hbar^3}\sum P_{1,3}(j,l;\omega_1,\omega_3)\sum P_{-\sigma,2}(i,k;-\omega_\sigma,\omega_2) \\ &\times\sum_{m\neq g}\sum_{n\neq g}\frac{\langle g|\mu_i|m\rangle\langle m|\bar{\mu}_k|f\rangle\langle f|\bar{\mu}_l|n\rangle\langle n|\mu_j|g\rangle}{(\omega_{gm}-\omega_\sigma)(\omega_{gf}-\omega_1-\omega_3-i\Gamma_{gf}/2)(\omega_{gn}-\omega_1)} \\ &= \frac{1}{6\hbar^3}\left[\sum P_{-\sigma,2}(i,k;-\omega_\sigma,\omega_2)\sum_m\frac{\langle g|\mu_i|m\rangle\langle m|\mu_k|f\rangle}{(\omega_{gm}-\omega_\sigma)}\sum P_{1,3}(j,l;\omega_1,\omega_3)\right. \\ &\left.\times\sum_n\frac{\langle f|\mu_l|n\rangle\langle n|\mu_j|g\rangle}{(\omega_{gn}-\omega_1)}\right]\frac{1}{(\omega_{gf}-\omega_1-\omega_3-i\Gamma_{gf}/2)} \\ &= \frac{1}{6\hbar}S_{ik}S_{lj}^*\frac{1}{(\omega_{gf}-\omega_1-\omega_3-i\Gamma_{gf}/2)} \end{aligned} \tag{10}$$

where $\omega_1 = \omega_3 = \omega$, $\omega_2 = -\omega$ and $\omega_\sigma = \omega_1 + \omega_2 + \omega_3 = \omega$ in the case of a degenerate 2PA process. In the last step of Eq. (10), it was introduced the two-photon transition matrix element S, defined by

$$S_{ik} = \frac{1}{\hbar}\sum_m\left[\frac{\langle g|\mu_i|m\rangle\langle m|\mu_k|f\rangle}{(\omega_{gm}-\omega_\sigma)}+\frac{\langle g|\mu_k|m\rangle\langle m|\mu_i|f\rangle}{(\omega_{gm}-\omega_\sigma)}\right] \tag{11}$$

For a degenerate 2PA process, the nonlinear absorption at the angular frequency ω of the incident laser light can now be rewritten as

$$\sigma_{2PA}(\omega) = \frac{8\pi^2\omega^2}{n^2c^2}L^4\sum_{f\neq g}\delta_{gf}\frac{(\Gamma_{gf}/2)}{(\omega_{gf}-2\omega)^2+(\Gamma_{gf}/2)^2} \tag{12}$$

where δ_{gf} is the 2PA transition probability for the electronic transition between the ground (g) and a final (f) excited state. The 2PA transition probability is calculated considering the orientational average of S and in the case of a linearly polarized excitation laser beam is given by

$$\delta_{gf} = \frac{1}{15}\sum_{i,j=x,y,z}(S_{ii}S_{jj}^{*} + S_{ij}S_{ij}^{*} + S_{ij}S_{ji}^{*}) \tag{13}$$

In order to describe the 2PA of a system through a broad spectral region we must consider the spectral line shape of the two-photon resonances. Adopting a normalized Lorentzian function to describe the spectral line shape of such resonances the Eq. (7) can then be written as

$$\sigma_{2PA}(\omega) = \frac{8\pi^3\omega^2}{n^2c^2}L^4\sum_{f\neq g}\delta_{gf}g(\omega_{gf} - 2\omega; \Gamma_{gf}/2) \tag{14}$$

The first approach assumes the two-photon resonant conditions to simulate the spectrum and therefore we denote it as "resonant expression" (RE) method. In this case the simulated 2PA cross-section spectrum is given by

$$\sigma_{2PA}(\omega) = \frac{8\pi^3\omega^2}{n^2c^2}L^4\sum_{f\neq g}^{N_{fs}}\left[\frac{1}{N_c}\sum_{k}^{N_c}\delta_{gf}^{k}g(\omega_{gf}^{k} - 2\omega; \Gamma_{gf}/2)\right] \tag{15}$$

In Eq. (15) N_c is the number of uncorrelated configurations sampled and N_{fs} the number of final electronic states considered to simulate the 2PA cross-section spectrum. The superscript k refers again to the kth uncorrelated configuration sampled. The term in the brackets is the average 2PA transition probability of a given transition of the system studied.

The second approach does not assume resonant conditions and it is based on the application of Eqs. (5)–(8). Therefore, we denote it as the "full expression" (FE) method. In this case the simulated 2PA cross-section spectrum is given by Eq. (16), where $\gamma^{k}(-\omega; \omega, -\omega, \omega)$; is defined by Eq. (8).

$$\sigma_{2PA}(\omega) = \frac{8\pi^2\hbar\omega^2}{n^2c^2}L^4\sum_{f\neq g}^{N_{fs}}\left[\frac{1}{N_c}\sum_{k=1}^{N_c}\mathrm{Im}[\langle\gamma^{k}(-\omega;\omega,-\omega,\omega)\rangle]\right] \tag{16}$$

It is worth to note that the FE method describes the second-order hyperpolarizability of a given molecular system for any incident radiation angular frequency. Therefore, the degenerate 2PA spectrum can be determined by scanning the incident radiation angular frequency ω along the desired spectral region. Unfortunately, the high amount of electronic states needed to obtain converged results makes such method time consuming, in contrast to the RE method. On the other hand, the FE method provides a more precise description of the 2PA transitions and, therefore, its application in this work provides the opportunity of shedding light on and assessing the description provided by the RE method.

In the last few years, many studies on the 2PA of molecules in gas phase or solvent adopting the PCM method [36–38] have been carried out. In these cases spectroscopic calculations were performed adopting a single molecular conformation for the solute molecule. These studies have either employed the definition of the 2PA cross-section adopted here by the FE method (Eq. (16)) and INDO/CI calculations [57–61,83] or the definition adopted in the RE method (Eq. (15)) and *ab initio* CI calculations to compute 2PA spectra [84,85]. Therefore, to the best of your knowledge this work also represents the first report on the performance differences between these two approaches used to describe 2PA spectra.

Quantum chemical calculations

The spectroscopic calculations were all performed using the Zerner's intermediate neglect of differential overlap (ZINDO) method with the ZINDO program package [86]. It uses the INDO/S Hamiltonian [87] and the Matagá-Nishimoto empirical two-electron integrals [88]. INDO/CIS and INDO/CISD calculations were performed to study the absorption processes of FSD in water. The Sum-Over-States (SOSs) model [56] was used to describe the 2PA process and computations including 50, 100, 150, 200 and 250 electronic transitions were performed to verify the convergence of the results. The CI-active space was restricted to the 40 highest-occupied and 40 lowest-unoccupied molecular orbitals for singly excited configurations calculations (CIS). In the case of CISD calculations, the same CI-active space was considered for the singly excited configurations and the 2 highest-occupied and 2 lowest-unoccupied molecular orbitals were considered for doubly excited configurations.

It is known that the original ZINDO program [86] by Zerner has been parameterized using INDO/CIS and properly describes electronic transitions of single excitation character. In general, it describes the 1PA spectra of organic molecules with good precision. However, to properly describe 2PA spectra one has to consider double excitation configurations. Therefore, in this work we have performed both CIS and CISD calculations for two reasons. The doubly excited configurations considered here are important for the SOS model, but has only a minor effect on the low-lying single excitations. Hence, in one hand, we verify the effect of the doubly excited configurations in the description of the 2PA spectrum of FSD and in the other we determine possible undesired effects on its 1PA spectrum. For all the computation performed in the present study we set the damping constants (Γ) equal to 0.2 eV for all excited states. This is a typical value adopted for organic molecules [57]. All the SOS calculations of the two-photon processes were made using the program Photon2 recently developed [89].

Finally, for comparison purpose time dependent density functional theory (TD-DFT) [90–92] calculations were performed for the two simplest solvent models (isolated FSD and FSD in an electrostatic embedding) and also employing the PCM method [36–38]. The TD-DFT calculations used the B3LYP/6-311++G(d,p) level [77,78] for describing the 1PA process of FSD in water, as implemented in the Gaussian 03 package [79]. The results of INDO/CI and TD-DFT calculations for the energy and solvatochromic shift of the lowest and most intense 1PA transition of FSD in water are compared.

Results and discussion

Analysis and solvent models

Using the S-QM/MD methodology, a set of 250 statistically relevant (uncorrelated) configurations composed by the solute and several solvent molecules were sampled from the classical simulation for *a posteriori* quantum mechanical (QM) calculations. The distribution of water molecules around the solute FSD is here discussed based on the concept of solvation shells, which are obtained applying a radial distribution function (RDF). Among several possibilities, the RDF between the center-of-mass of the solute and solvent molecules is probably the most usual. However, it has been showed that such RDF is not appropriate when the solute has a general form. Therefore, to analyze the solvation shells of FSD in water we choose the minimum-distance distribution function [93,94]. This is shown in Fig. 2, where at least three peaks can easily be identified. Volume integration of the distribution function gives the coordination number of each peak. This is the number

of water molecules around the solute, and so, determines the size of each solvation shell. The first peak is composed by the first 14 water molecules, most of them making hydrogen bonds with the solute molecule. Therefore, throughout this work we refer to it as a "hydrogen bond" shell. These molecules do not actually compose a solvation shell because they do not completely surround the FSD. In this sense, the first solvation shell is defined by the first 47 water molecules.

The linear and nonlinear absorption of FSD in water is calculated using six distinct (discrete and explicit) solvent models. In the model 1, the QM calculations were performed for the isolated FSD molecule. In the model 2, the configurations are composed by FSD embedded in the electrostatic field of 500 water molecules. These 500 water molecules are located within a radial distance of 11.3 Å from the FSD's center-of-mass. In the model 3, the configurations are composed by FSD + 14 explicit water molecules (the "hydrogen bond" shell). The model 4 is composed by the model 3 with the inclusion of the electrostatic embedding of all 486 remaining water molecules within the same radial distance. In the model 5 the configurations are composed by FSD + 47 explicit water molecules (the first solvation shell). And finally, the model 6 is composed by the model 5 embedded in the electrostatic field of all 453 remaining water molecules. In the models 5 and 6 the configurations include 176 atoms and 498 valence electrons, justifying the use of a semi-empirical approach in particular for studying the 2PA absorption process. The results obtained for the six models adopted in this study are verified to be statistically converged. Moreover, in Fig. 2 one can also identify a second solvation shell composed by 90 water molecules. In the present study we did not perform QM calculations explicitly considering such solvation shell. This would be costly even for a semi-empirical approach, since studying the 2PA demands a large amount of electronics transitions to be included into the SOS model. However, the results obtained with the model 6 seem to be converged with respect to the number of explicit solvent molecules.

The MD simulation was performed keeping both FSD and solvent molecules flexible. The main change observed on the conformation of FSD was the orientation of the phenyl carboxyl group during the classical simulation. The dihedral angle between phenyl carboxyl group and the single aromatic ring of FSD is defined by the atoms 15–16–21–22 (Fig. 1). Its average value and standard deviation was 85 ± 5°. Thus, during the classical simulation the phenyl carboxyl group remained almost perpendicular to the single aromatic ring of FSD. It is worth to mention that this average angle is different from the one observed on the initial optimized geometry (from QM calculation), for which the dihedral angle was 3°. Moreover, only a very small fluctuation (91 ± 3°) was observed for the dihedral angle between the single aromatic ring of FSD and its xanthene ring portion, defined by atoms 3–7–15–16 (Fig. 1).

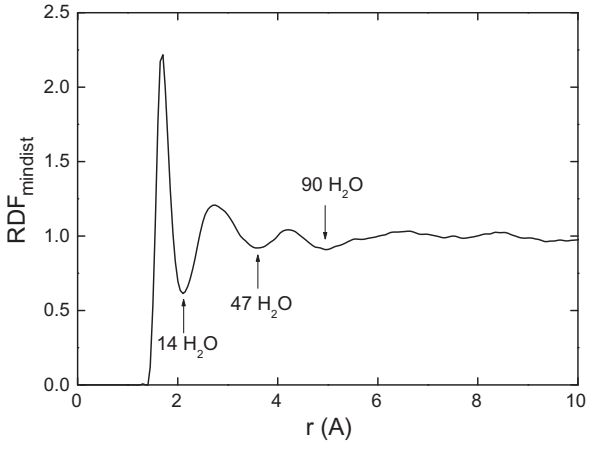

Fig. 2. Solvation shells of FSD in water obtained from the minimum-distance radial distribution function ($RDF_{mindist}$).

One-photon absorption

The 1PA cross-section spectrum of FSD was determined calculating the 20 lowest electronic transitions. The energy of the lowest and most intense $\pi \rightarrow \pi^*$ transition was used to confirm the statistical convergence of the results for all six distinct solvent models. Fig. 3 shows the convergence of the INDO/CIS and INDO/CISD calculations for both the simplest and the most realistic solvent models adopted in this study.

Table 1 gathers the INDO/CI results obtained for the energy of such $\pi \rightarrow \pi^*$ transition in this study, the results obtained in a previous study performed using Monte Carlo (MC) simulation and also experimental data available on the literature. In addition, the TD-DFT results obtained for isolated FSD, FSD in the electrostatic embedding of the solvent molecules and employing the PCM model are also presented for comparison purposes. Three important trends should be noted in the INDO/CI results. First, the INDO/CI calculations overestimate the energy of the $\pi \rightarrow \pi^*$ transition. This is expected due to the dianionic character of FSD and the limitations of the ZINDO method concerning the lack of diffuse basis set functions. Second, the flexibility of the FSD molecule in the MD simulation improved the theoretical results in comparison to the previous work. Third, the inclusion of double excitations (INDO/CISD) slightly changes the energy of the $\pi \rightarrow \pi^*$ transition. It worsens the description of the solvatochromic shift of the $\pi \rightarrow \pi^*$ transition, however the unusual direction of this shift remains correctly reproduced.

The difference between the INDO/CI results for the energy of the $\pi \rightarrow \pi^*$ transition of FSD in water and the experimental data is about 0.20 eV and it should not be overlooked. However, the INDO/CI calculations provide a better description of the lowest-energy transition of FSD than the TD-DFT, for both FSD isolated and in the electrostatic embedding. Moreover, the TD-DFT method obtains the solvatochromic shift in water in the wrong direction. Based on these two aspects, we conclude that INDO/CI calculations represent an interesting and convenient option to study the spectroscopic behavior of FSD in water.

The $\pi \rightarrow \pi^*$ character of the lowest energy transition of FSD in water is confirmed by the molecular orbitals involved in such transition, determined at the INDO/CI level. The transition is mostly described by an excitation from the highest occupied molecular orbital (HOMO) to the lowest unoccupied molecular orbital (LUMO). These molecular orbitals are showed in the Fig. 4.

The 1PA and 2PA spectra of FSD in water along a broad spectral region were reported by Makarov and co-workers [33] and are illustrated in Fig. 5. The experimental 1PA spectrum of FSD in water shows that the band centered at 490 nm, ascribed to the lowest energy $\pi \rightarrow \pi^*$ transition, presents a shoulder possibly related to another electronic transition close in energy to the lowest one. However, the INDO calculations, both CI and CISD, indicate that the energy of the second lowest transition of FSD in water is about 1 eV higher than the lowest one. On the other hand, theoretical calculations of the vibrational modes of FSD in its electronic ground state indicate that the molecule has an intense mode at the 1700 cm^{-1}. Therefore this shoulder should be more correctly ascribed to the first term of a vibrational progression.

As it was already mentioned here, the original ZINDO program [86] was parameterized using the INDO/CIS calculations to properly describes electronic transitions of single excitation character and it satisfactorily describes 1PA spectra in general. Therefore, it is expected that the inclusion of double excitations could compromise the description of the 1PA spectrum. Fig. 6 shows the 1PA

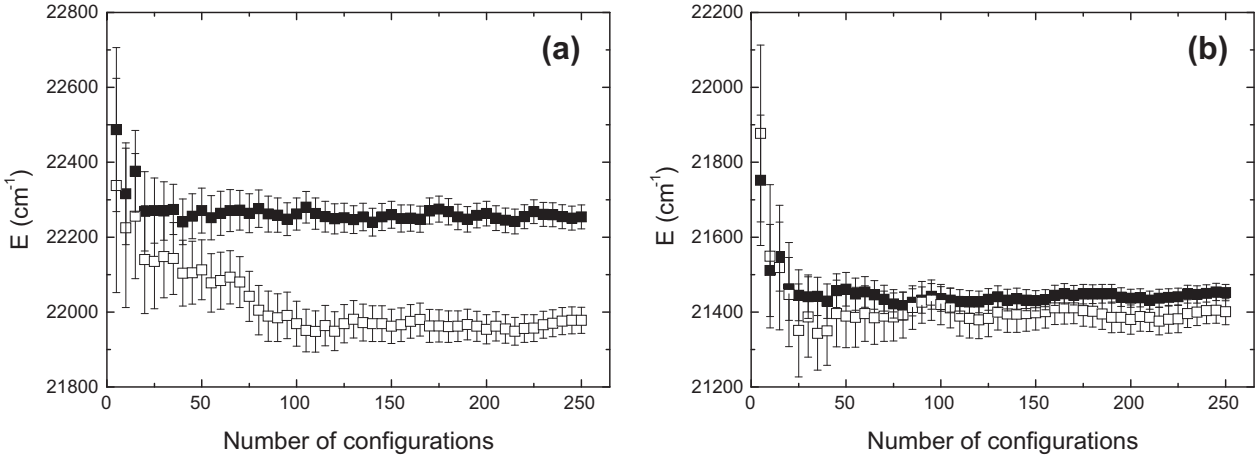

Fig. 3. Statistical convergence of the INDO/CIS (filled squares) and INDO/CISD (empty squares) results for the energy of the lowest and most intense one-photon transition, $\pi \rightarrow \pi^*$, of FSD in water. (a) Model 1: FSD isolated. (b) Model 6: FSD + explicit first solvation shell + electrostatic embedding.

Table 1
Energy and solvatochromic shift of the lowest and most intense one-photon transition of FSD in water obtained from QM calculations performed using uncorrelated configurations provided by classical simulations. The transition energy (E) is given by the transition wavelength in nanometer and the solvatochromic shift ($\Delta\nu$), in respect to the vacuum (FSD isolated), in cm^{-1}. The TD-DFT calculations were performed with the hybrid B3LYP functional and the 6-311++G(d,p) basis set. The results obtained employing PCM are presented in parentheses.

Model	MC simulation[a]				MD simulation							
	CIS		TD-DFT		CIS		CISD		TD-DFT		Exp.	
	E	$\Delta\nu$	*E*	$\Delta\nu$	*E*	$\Delta\nu$	*E*	$\Delta\nu$	*E*	$\Delta\nu$	E^b	$\Delta\nu^c$
FSD isolated	449	–	430	–	471	–	467	–	430	–	490	+1150
FSD + embedding	432	+875	432 (437)	−108 (−370)	447	+1140	433	+1680	437 439	−370 (−477)		
FSD + 14 H2O + embedding	433	+845			453	+845	452	+710				
FSD + 47 H2O + embedding	433	+840			452	+890	456	+600				

[a] Previous work [52].
[b] Experimental data of FSD in water [31].
[c] Solvatocromic shift from anhydrous DMSO to water [31].

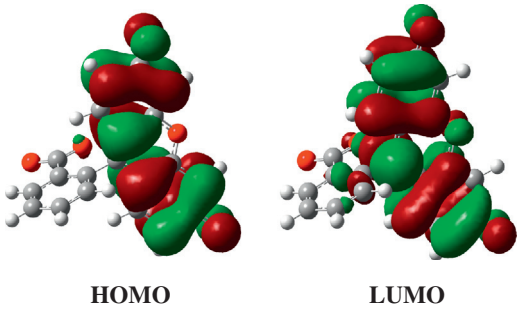

Fig. 4. Molecular orbitals involved in the lowest energy transition ($\pi \rightarrow \pi^*$) of FSD in water.

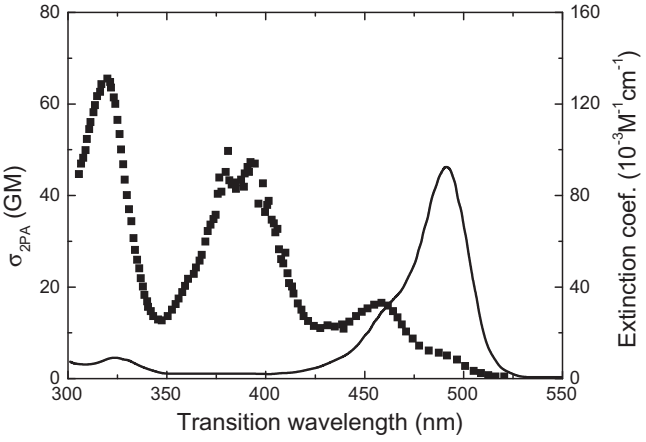

Fig. 5. 1PA spectrum (ε: extinction coefficient; continuum line) and the 2PA spectrum (σ_{2PA}: black squares) of FSD in water. Experimental spectra were digitized from a work reported by N.S. Makarov and co-workers [33].

cross-section spectrum simulated using the results provided by the CIS and CISD calculations for four of our solvent models. The experimental 1PA spectrum of FSD in water is basically composed by two bands at the UV–Vis region, the band related to the $\pi \rightarrow \pi^*$ transition and a small band around 325 nm. Both bands appear at the simulated 1PA spectra, Fig. 6, but in relation to the experimental spectrum they are blue shifted about 40–50 nm.

Fig. 6 shows that the inclusion of double excitations in the INDO/CI calculations performed by the ZINDO program does not compromise the description of the 1PA spectrum of FSD. The inclusion of double excitation diminishes the 1PA cross-section of the lowest energy $\pi \rightarrow \pi^*$ transition by about 25%, while the solvent effects do not change it substantially. The opposite is observed for the higher energy region of the 1PA spectrum. The solvent effect completely inhibits a small band around 350 nm in the spectrum of FSD isolated and which does not appear in the experimental spectrum. The inclusion of double excitations basically does not change the amplitude of the band centered around 275 nm. This band in the simulated spectra is related to the small

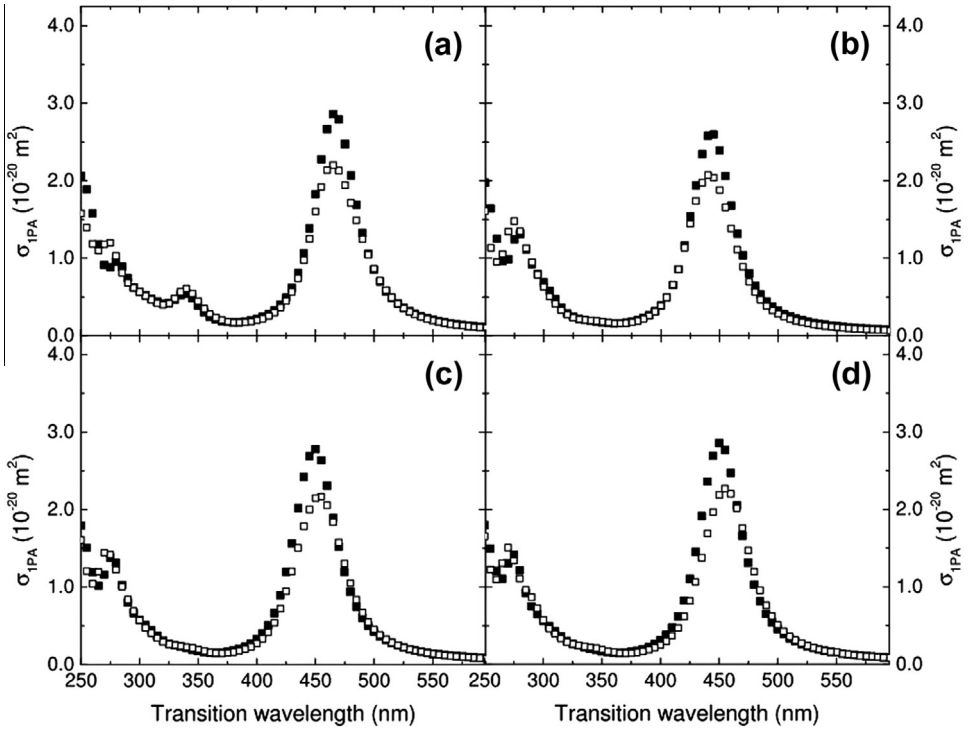

Fig. 6. 1PA cross-section spectrum of FSD simulated using the results provided by the INDO/CIS (■) and INDO/CISD (□) calculations. (a) FSD isolated, (b) FSD in an electrostatic embedding, (c) FSD surrounded by 14 explicit water molecules and including the electrostatic embedding, (d) FSD surrounded by whole first solvation shell (47 explicit water molecules) included explicitly and including electrostatic embedding.

band around 325 nm in the experimental spectrum. The amplitude of this band is overestimated by the INDO/CI calculations in all solvent models adopted in this work.

Two-photon absorption

To employ the SOS model to study the 2PA, it is necessary first to investigate the convergence of the theoretical results in relation to the number of the excited states taken into account in such model. Since we studied the solvent effects on the 2PA of FSD in aqueous environment using six different solvent models, we investigated the convergence for each model. In Fig. 7, we present the results obtained for two of them, FSD isolated and FSD surrounded by 14 explicit water molecules ("hydrogen bond" shell) with the electrostatic embedding. The computations took into account 50, 100, 150, 200 and 250 excited states. The results are the average values of the imaginary part of $\gamma(-\omega;\omega,-\omega,\omega)$ (i.e., Im[$\gamma(-\omega;\omega,-\omega,\omega)$]) at the two-photon resonance frequencies ($\omega = \omega_{gf}/2$) obtained taking the 250 uncorrelated configurations coming from the classical simulation and employing the FE method, Eq. (8).

From Fig. 7, it is seen that the inclusion of double excitations in the INDO/CI calculations considerably changes Im[$\gamma(-\omega;\omega,-\omega,\omega)$], mainly at the higher energy spectral region. This was observed not only for the two models shown on Fig. 7, but also for the four remaining models (not shown). The number of two-photon resonances ($\omega = \omega_{gf}/2$), before Im[$\gamma(-\omega;\omega,-\omega,\omega)$] drops to zero, due to the one-photon resonance approximation, diminishes with the inclusion of double excitations. Also, the convergence of the results in relation to the number of excited states is slower for the INDO/CISD calculations. When using the INDO/CIS results, the SOS model already provided converged values for computations including 50 states, while to obtain converged values using the INDO/CISD results at least 100 states are needed. Therefore, to simulate the 2PA spectrum of FSD in water we took into account 150 excited states in the SOS model. Comparing the values obtained for Im[$\gamma(-\omega;\omega,-\omega,\omega)$], the values estimated using the INDO/CIS results at the region of higher energy excited states are at least one order of magnitude higher than the values estimated using the INDO/CISD results. From the experimental values reported [33] it is known that the 2PA cross-section of FSD in water along the visible and near-ultraviolet region is few tens Göppert–Mayer (1GM = 10^{-50} cm^4 s photon^{-1}). Through the Eq. (7), one can realize that for such values of cross-sections the magnitude of Im[$\gamma(-\omega;\omega,-\omega,\omega)$] should be about 10^5–10^6 a.u. Therefore, the INDO/CIS calculations provide overestimated values at the region of the higher energy excited states. These results confirm the initial hypothesis that for a proper determination of the 2PA cross-section spectrum using INDO/CI calculations it is necessary to include double excitations. Based on this conclusion, from now on we will be presenting and discussing here only the results obtained from INDO/CISD calculations.

As exposed on the procedure section, in this work we simulated the 2PA cross section spectrum of FSD in water employing the semi-classical method to simulate absorption spectra and adopting two different approaches, the RE and FE methods, to describe the nonlinear absorption process. While the RE method estimates Im[$\gamma(-\omega;\omega,-\omega,\omega)$] at the two-photon resonant frequencies ($\omega = \omega_{gf}/2$) taking into account only the two-photon resonant terms of the SOS model (Eq. (10)), the FE method does not neglect any term of the SOS model (Eq. (8)). Since the 2PA cross-section is proportional to the imaginary part of $\gamma(-\omega;\omega,-\omega,\omega)$, this is the only difference between the methods used to simulate the 2PA cross-section spectrum. Fig. 8 shows the values of Im[$\gamma(-\omega;\omega,-\omega,\omega)$] at the two-photon resonant frequencies computed for all six solvent models and employing the two approaches. The results shown are the average values (and the standard deviations) for each two-photon resonance frequency for 250 uncorrelated configurations.

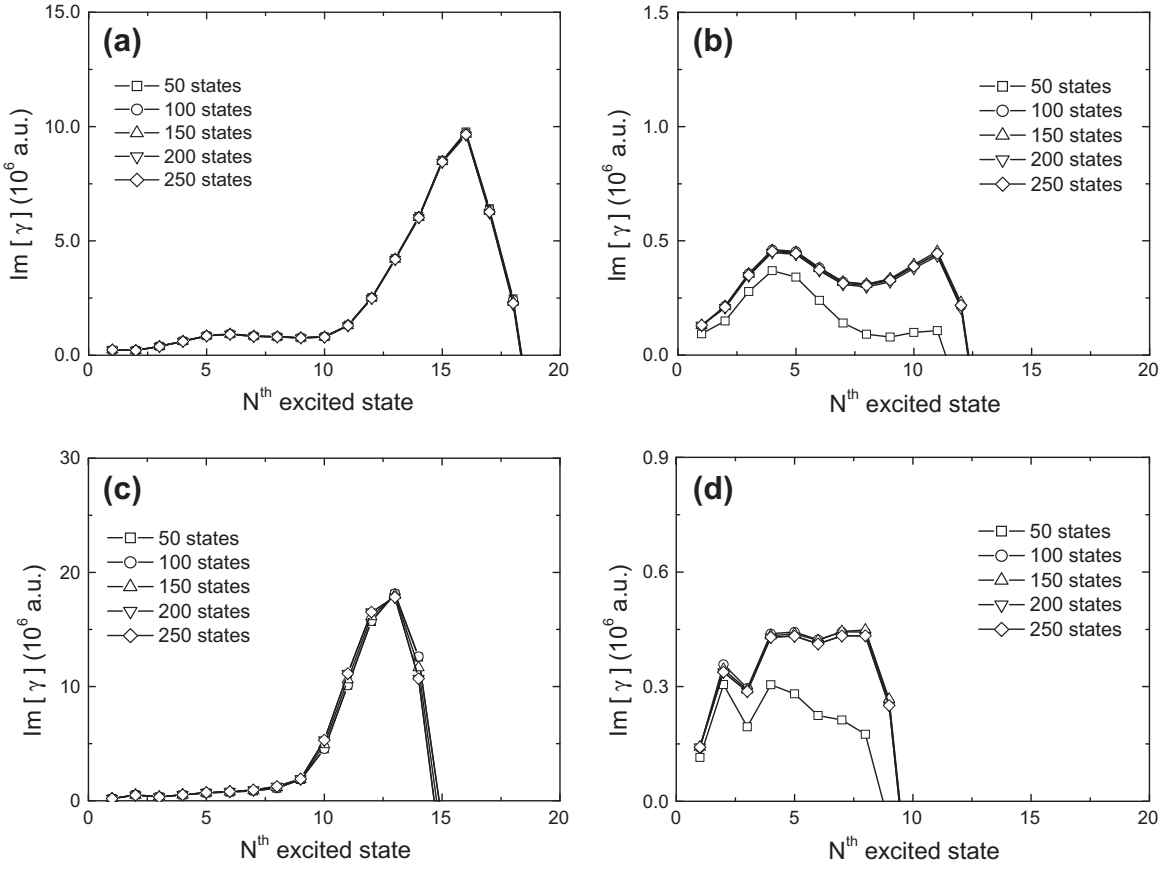

Fig. 7. Results provided by the SOS model for the imaginary part of $\gamma(-\omega; \omega, -\omega, \omega)$ as a function of the number of electronic states included in the summation for the two models adopted in this study. (a) FSD isolated and INDO/CIS calculation, (b) FSD isolated and INDO/CISD calculation, (c) FSD + 14 explicit solvent molecules + electrostatic embedding and INDO/CIS calculation and (d) FSD + 14 explicit solvent molecules + electrostatic embedding and INDO/CISD calculation.

From Eqs. (8) and (10) one can note that the FE and RE do not describe the effect of the one-photon resonance approximation over Im[$\gamma(-\omega; \omega, -\omega, \omega)$] in a similar way. When the angular frequency of the incident light increases and approaches the angular frequency of the lowest one-photon resonance, in the FE method Im[$\gamma(-\omega; \omega, -\omega, \omega)$] quickly drops to zero and then becomes negative. In the RE method on the other hand, the value of Im[$\gamma(-\omega; \omega, -\omega, \omega)$] suffers a resonant enhancement effect in such situation. Both methods do not give a correct dispersion behavior of Im[$\gamma(-\omega; \omega, -\omega, \omega)$] at the frequency region around the one-photon resonance, since they are based on the SOS model which fails in this aspect [95]. However, it is easier to identify the effects of the one-photon resonance approximation from the trend observed on the results of the FE method. Therefore, in the present study such trend was used to define the number of final excited states (N_{fs}) to be adopted to simulate the 2PA cross-section spectrum employing both methods. This procedure inhibits the action of resonant enhancement effects over the simulated nonlinear spectrum provided by the RE method. Based on the results presented on Fig. 8, the 12 lowest electronic excited states were used as final excited states to simulate the 2PA cross-section spectrum of isolated FSD. The inclusion of the solvent reduced this number and for the five remaining models the 9 lowest electronic excited states were used.

Fig. 8 shows that the two methods proved similar results to the first excited state for all solvent models. For model 1, FSD isolated, the values of Im[$\gamma(-\omega; \omega, -\omega, \omega)$] estimated by the FE method is higher, twice for several excited states, than the values estimated by the RE method. Similar trend is also observed for the model 2. For all the remaining models, the value of Im[$\gamma(-\omega; \omega, -\omega, \omega)$] estimated with the RE method for the third until the eighth excited states is about 50–80% of the values estimated with the FE method, being the second excited state the only exception. A direct comparison of the results provided by the two methods for the last excited state adopted to simulate the nonlinear spectra in each model is not possible, since a residual effect of the one-photon resonance approximation is certainly affecting such value in a distinct way for each method.

Fig. 9 presents the simulated 2PA cross-section spectra of FSD in water for the six solvent models adopted in this study. Three bands can be clearly identified in the experimental 2PA cross-section spectrum of FSD, Fig. 5. In this way, here the simulated nonlinear spectra are mainly discussed considering the amplitude and position of the bands which appeared along the UV–Vis spectral region. Fig. 8 evidences the number of final excited states playing at the different spectral regions (visible and near ultraviolet) along the nonlinear absorption spectrum of FSD in water.

The 2PA spectra provided by both methods indicate that the amplitude of the first band, centered around 465 nm and related with the two-photon transition to the first excited state (dipolar transition), is not substantially affected by solvent effects. However, when the results of the models 1 (Fig. 9a) and 3 (Fig. 9c) are compared, it is possible to note that the hydrogen bonds slightly increase the 2PA cross-section of such transition. Moreover, comparing the results of the models 3 (Fig. 9c) and 4 (Fig. 9d), and also the models 5 (Fig. 9e) and 6 (Fig. 9f), it is possible to note that the electrostatic embedding slightly decreases this 2PA cross-section. The experimental value of the 2PA cross-section at 490 nm (the wavelength of the linear absorption peak) is 6 GM. The FE method estimates the amplitude of the first band (peak va-

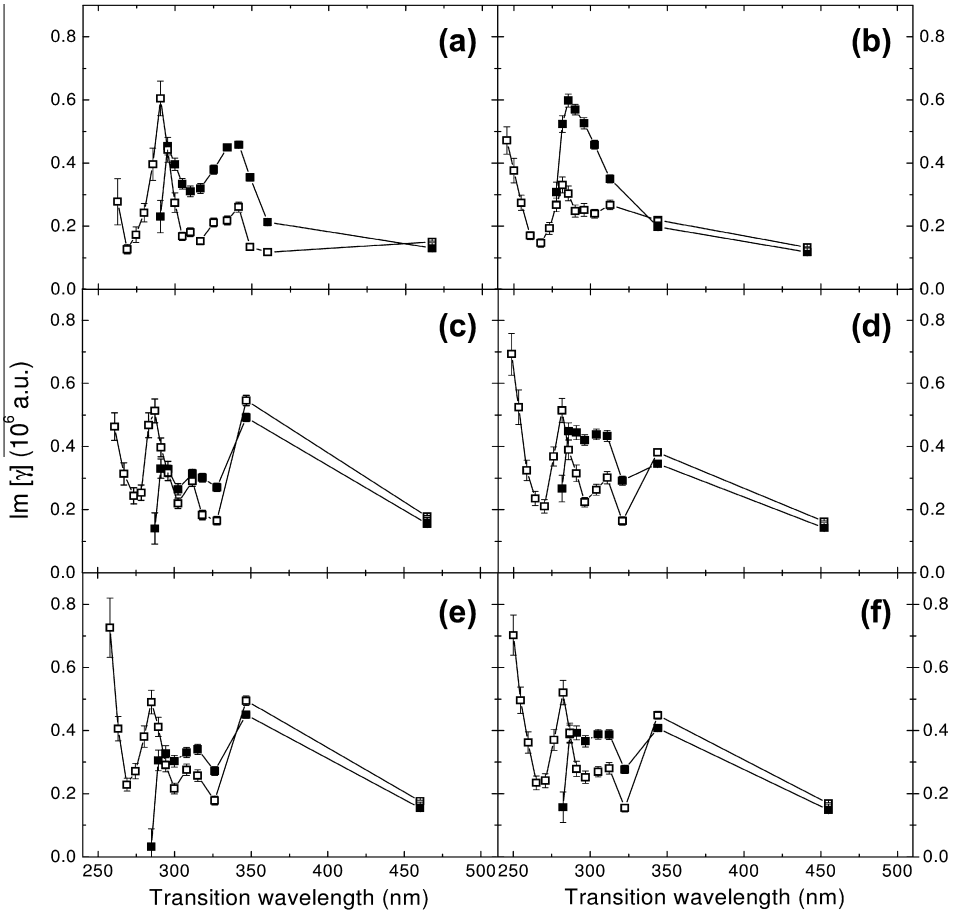

Fig. 8. Computed average values for Im[$\gamma(-\omega;\omega,-\omega,\omega)$] at the two-photon resonance frequencies employing the FE (■) and the RE (□) methods. (a) FSD isolated, (b) FSD in an electrostatic embedding, (c) FSD surrounded by 14 explicit solvent molecules ("hydrogen bond" shell), (d) FSD surrounded by 14 explicit solvent molecules and including electrostatic embedding, (e) FSD surrounded by 47 explicit water molecules (first solvation shell) and (f) FSD surrounded by 47 explicit water molecules and including electrostatic embedding.

lue) equal to 7 GM, but the RE method underestimates the amplitude of this band by about 50%.

The second band of the experimental 2PA spectrum is centered at 385 nm, while the third one, the most narrow and with larger amplitude ($\sigma_{2PA} \sim 65$GM), is centered at 320 nm. The 2PA spectrum provided by the FE method for FSD isolated is the simulated spectrum most similar to the experimental one. In this spectrum, the third band is centered around 295 nm and it has an amplitude of about 62 GM. The second band is centered around 335 nm with a peak amplitude of about 52 GM and a subtle shoulder. Since the QM calculations performed in this study do not include vibronic coupling, the observed shoulder has certainly electronic origin.

The interaction with explicit solvent molecules decreases the amplitude of the third band, but no solvatochromic shift is observed due to such interaction. When the electrostatic embedding is included in the explicit models the description provided by the FE method leads to an increase of the third band amplitude. Concerning the solvent effects on the third band of the nonlinear spectrum, all the predictions made by the FE method are reproduced by the RE method, however in a less evident way. The results found for the discrete (electrostatic) model is the only exception. The FE and RE methods provide similar amplitudes for the last band of the nonlinear spectrum and in good agreement with the experimental 2PA cross-section spectrum.

The solvent effect on the second band of the 2PA spectrum is the origin of the main changes observed in the entire nonlinear spectrum. The second band splits in two when explicit molecules are included. This is because the shoulder and the peak of the initial (FSD isolated) second band suffer solvatochromic shift in opposite directions. The shoulder shifts in the direction of the third band (blue shift) and, therefore, their amplitude could be added in a superposition effect if the shift were large enough. However, its position seems to be already established in the case of the most sophisticated solvent model used in this study and the superposition is not observed. Moreover, analyzing only the part of the initial second band which shifted to the red region, i.e., its peak (FSD isolated), it can be observed that both, the interaction with explicit solvent molecules and the one coming from the electrostatic embedding, diminishes the 2PA cross-section of FSD around that spectral region.

The identification of the second band and analysis of the solvent effects on it are more difficult when using the RE method for two reasons. First, the method underestimates the values of Im[$\langle\gamma(-\omega;\omega,-\omega,\omega)\rangle$] for the excited electronic states contributing to the amplitude of that band, as seen in Fig. 8. This makes this band to appear as less intense in these simulated 2PA spectra. Second, the FE and RE methods do not adopt exactly the same function to describe the excited states spectral lines. As it can be seem in the insets of Fig. 9, which highlight the lowest energy and isolated 2PA transition of FSD, the profile of each excited state spectral line is broader in the RE method. Finally, the FE and RE methods provide a very similar description concerning the solvent effects on the 2PA of FSD in water for most of the solvent models used in this work.

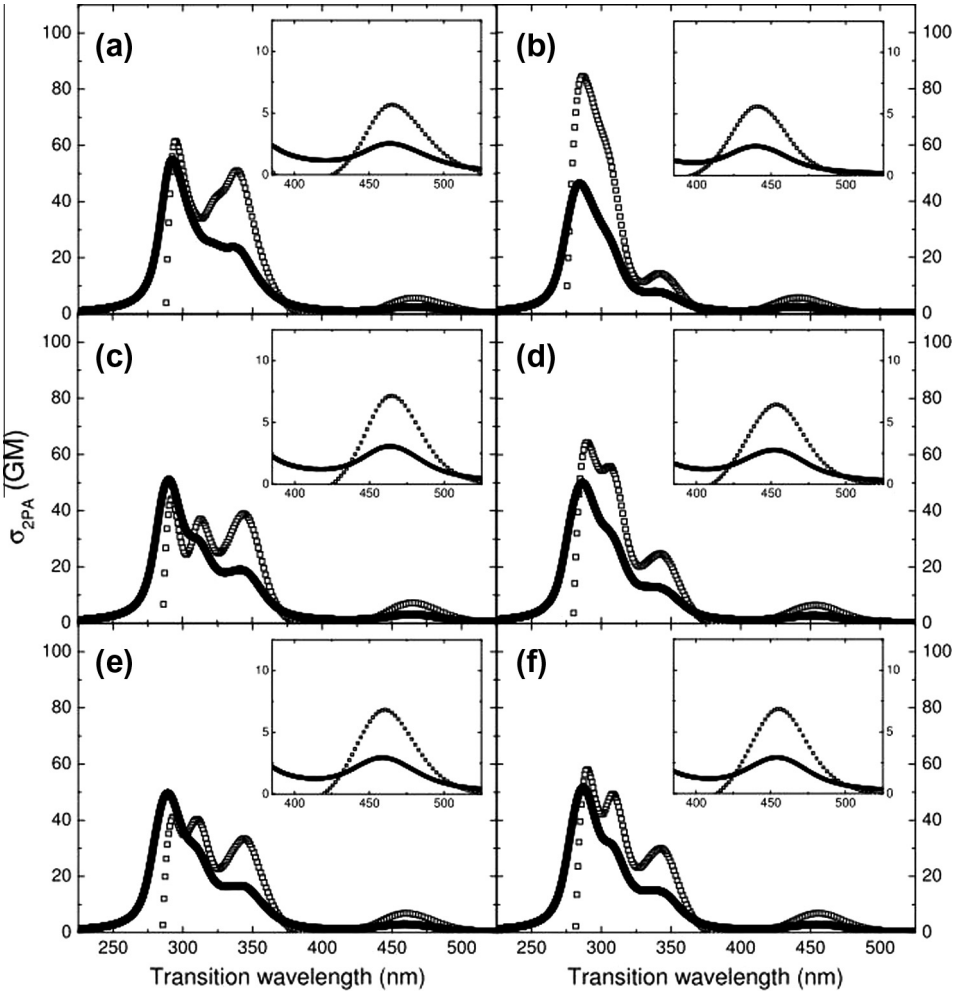

Fig. 9. 2PA cross-section spectrum of FSD in water simulated employing the FE (empty squares) and the RE (filled squares) methods. (a) FSD isolated, (b) FSD in an electrostatic embedding, (c) FSD surrounded by 14 explicit solvent molecules (“hydrogen bond” shell), (d) FSD surrounded by 14 explicit solvent molecules and including electrostatic embedding, (e) FSD surrounded by 47 explicit water molecules (first solvation shell) and (f) FSD surrounded by 47 explicit water molecules and including electrostatic embedding.

Summary and conclusions

The present work presents a theoretical study of the 1PA and 2PA cross-section spectra of FSD in water. Using a combined and sequential QM/MD methodology six different solvent models, explicit and discrete, were adopted to investigate in detail the role of solute – solvent interaction on the 1PA and 2PA of FSD in water. Statistically uncorrelated configurations were sampled from the MD simulation for *a posteriori* quantum mechanical calculations using the ZINDO method. INDO/CIS and INDO/CISD calculations were performed to study the absorption processes of FSD and the SOS model used to describe the 2PA process. The 1PA and 2PA spectra of FSD in water were simulated employing the semi-classical method to simulate the absorption spectra. In the case of the 2PA, the nonlinear spectrum was simulated using two approaches, the “full expression” (FE) and the “resonant expression” (RE) methods. The last method assumes the two-photon resonant conditions and represents an interesting computation option to study the 2PA process.

The inclusion of double excitations does not affect the description of the 1PA of FSD in water along the visible and near ultraviolet spectral regions. The simulated 1PA spectrum indicates that the main effect of the solvent environment on the linear spectrum of FSD in water is to inhibit a small band around 340 nm which appeared in the spectrum of the FSD isolated. The spectral profile of the 1PA cross-section spectrum obtained using any of the solvent models adopted in this work is in good agreement with the experimental spectrum. However, the simulated 1PA spectra are blue shifted in about 40–50 nm in comparison to the experimental spectrum. The direction of the unusual blue shift of the lowest-energy and most intense 1PA transition playing over the linear spectrum of FSD, a $\pi \rightarrow \pi^*$ transition, is properly described by the INDO/CI calculations. The performance of the INDO/CI and TD-DFT methods were compared for three cases, isolated FSD, FSD in an electrostatic embedding and using the PCM model. In all cases the INDO/CI calculations provided better results for the wavelength and solvatochromic shift of the $\pi \rightarrow \pi^*$ transition.

In the case of 2PA process, the introduction of doubly excited configuration interactions (INDO/CISD) proved to be essential for an appropriate description of the process at the higher energy spectral region. Despite the number of coordinations of FSD in water, it was observed that the solvent effects do not considerably change the 2PA cross-section along the entire nonlinear spectrum. The 2PA spectrum provided by the FE method presents a better definition of the bands which appear in the experimental spectrum than the one provided by the RE method. Nevertheless, both approaches provide similar description for the effect of the solvent environment on the 2PA transitions of FSD in water. In this sense,

considering the reduced computation cost of the RE method, this approach appears as an interesting option to study the solvent effect on the two-photon transitions of solvated molecules in a microscopy details.

Acknowledgments

This work has been partially supported by INCT-GFCx, NbioNet, CNPq, CAPES and FAPESP (Brazil).

References

[1] R.W. Boyd, Nonlinear Optics, third ed., Academic Press, London, UK, 2008.
[2] G.P. Agrawal, R.W. Boyd (Eds.), Contemporary Nonlinear Optics, Academic Press, New York, 1992.
[3] P.N. Prasad, D.J. Willians, Introduction to Nonlinear Optical Effects in Molecules and Polymers, Wiley-Interscience, New York, 1991.
[4] D.A. Parthenopoulos, P.M. Rentzepis, Science 245 (4920) (1989) 843–845.
[5] D.A. Parthenopoulos, P.M. Rentzepis, J. Appl. Phys. 68 (11) (1990) 5814–5818.
[6] W. Denk, J.H. Strickler, W.W. Webb, Science 248 (4951) (1990) 73–76.
[7] G.S. He, R. Gvishi, P.N. Prasad, B.A. Reinhardt, Opt. Commun. 117 (1–2) (1995) 133–136.
[8] G.S. He, J.D. Bhawalkar, C.F. Zhao, C.-K. Park, P.N. Prasad, Opt. Lett. 20 (23) (1995) 2393–2395.
[9] J.D. Bhawalkar, G.S. He, C.-K. Park, C.F. Zhao, G. Ruland, P.N. Prasad, Opt. Commun. 124 (1–2) (1996) 33–37.
[10] J.D. Bhawalkar, G.S. He, P.N. Prasad, Rep. Prog. Phys. 59 (9) (1996) 1041–1070.
[11] R.H. Köhler, J. Cao, W.R. Zipfel, W.W. Webb, M.R. Hansen, Science 276 (5321) (1997) 2039–2042.
[12] J. Oberle, L. Bramerie, G. Jonusauskas, C. Rulliere, Opt. Commun. 169 (1–6) (1999) 325–332.
[13] B. Herman, X.F. Wang, P. Wodnicki, A. Perisamy, N. Mahajan, G. Berry, G. Gordon, in: W. Retting, B. Strehmel, S. Schrader, H. Seifert (Eds.), Applied Fluorescence in Chemistry Biology and Medicine, Springer, New York, 1999, pp. 491–507.
[14] K.D. Belfield, X.B. Ren, E.W. Van Stryland, D.J. Hagan, V. Dubikovski, E.J. Meisak, J. Am. Chem. Soc 122 (6) (2000) 1217–1218.
[15] S. Kawata, H.B. Sun, T. Tanaka, K. Takada, Nature 412 (6848) (2001) 697–698.
[16] J.A. Thomas, R.N. Buchsbaum, A. Zimniak, E. Racker, Biochemistry 18 (11) (1979) 2210–2218.
[17] S.G. Stanton, A.B. Kantor, A. Petrossian, J.C. Owicki, Biochim. Biophys. Acta 776 (2) (1984) 228–236.
[18] J. Hadjianestis, J. Nikokavouras, J. Photochem. Photobiol. A 69 (3) (1993) 337–343.
[19] M.E. Mummert, E.W. Voss, Mol. Immunol. 32 (16) (1995) 1225–1233.
[20] M. Bailey, P. Hagmar, D.P. Millar, B.E. Davidson, G. Tong, J. Haralambidis, W.H. Sawyer, Biochemistry 34 (48) (1995) 15802–15812.
[21] H. Kojima, K. Sakurai, K. Kikuchi, S. Kawahara, Y. Kirino, H. Nagoshi, Y. Hirata, T. Nagano, Chem. Pharm. Bull. 46 (2) (1998) 373–375.
[22] R. Sjoback, J. Nygren, M. Kubista, Spectrochim. Acta, Part A 51 (6) (1995) L7–L21.
[23] T. French, P.T.C. So, D.J. Weaver Jr., T. Coelho-Sampaio, E. Gratton, E.W. Voss Jr., J. Carrero, J. Microsc. 185 (1997) 339–353.
[24] D.W. Piston, S.M. Knobel, Methods Enzymol. 307 (1999) 351–368.
[25] P.T.C. So, C.Y. Dong, B.R. Masters, K.M. Berland, Annu. Rev. Biomed. Eng. 2 (2000) 399–429.
[26] G.H. Patterson, D.W. Piston, Biophys. J. 78 (4) (2000) 2159–2162.
[27] V. Zanker, W. Peter, Chem. Ber. Recl. 91 (3) (1958) 572–580.
[28] M.M. Martin, L. Lindqvist, J. Lumin. 10 (6) (1975) 381–390.
[29] N. Klonis, W.H. Sawyer, J. Fluoresc. 6 (3) (1996) 147–157.
[30] M.M. Martin, Chem. Phys. Lett. 35 (1) (1975) 105–111.
[31] N. Klonis, A.H.A. Clayton, E.W. Voss, W.H. Sawyer, Photochem. Photobiol. 67 (5) (1998) 500–510.
[32] M.A. Albota, C. Xu, W.W. Webb, Appl. Opt. 37 (31) (1998) 7352–7356.
[33] N.S. Makarov, M. Drobizhev, A. Rebane, Opt. Express 16 (6) (2008) 4029–4047.
[34] V.R. Batistela, J. da Costa Cedran, H.P. Moises de Oliveira, I.S. Scarminio, L.T. Ueno, A. Eduardo da Hora Machado, N. Hioka, Dyes Pigm. 86 (1) (2010) 15–24.
[35] P. Chandra Jha, Y. Wang, H. Agren, ChemPhysChem 9 (1) (2008) 111–116.
[36] S. Miertus, E. Scrocco, J. Tomasi, Chem. Phys. 55 (1) (1981) 117–129.
[37] B. Mennucci, J. Tomasi, J. Chem. Phys. 106 (12) (1997) 5151–5158.
[38] V. Barone, M. Cossi, J. Tomasi, J. Chem. Phys. 107 (8) (1997) 3210–3221.
[39] P.N. Day, K.A. Nguyen, R. Pachter, J. Chem. Phys. 125 (9) (2006) 094103.
[40] K. Zhao, L. Ferrighi, L. Frediani, C.-K. Wang, Y. Luo, J. Chem. Phys. 126 (20) (2007) 204509.
[41] K.A. Nguyen, P.N. Day, R. Pachter, J. Chem. Phys. 126 (9) (2007) 094303.
[42] Y. Zhao, A.-M. Ren, J.-K. Feng, X. Zhou, X.-C. Ai, W.-J. Su, Phys. Chem. Chem. Phys. 11 (48) (2009) 11538–11545.
[43] H.Y. Woo, J.W. Hong, B. Liu, A. Mikhailovsky, D. Korystov, G.C. Bazan, J. Am. Chem. Soc. 127 (3) (2005) 820–821.
[44] H.Y. Woo, D. Korystov, A. Mikhailovsky, T.-Q. Nguyen, G.C. Bazan, J. Am. Chem. Soc. 127 (40) (2005) 13794–13795.
[45] H.Y. Woo, B. Liu, B. Kohler, D. Korystov, A. Mikhailovsky, G.C. Bazan, J. Am. Chem. Soc. 127 (42) (2005) 14721–14729.
[46] Y. Tan, Q. Zhang, J. Yu, X. Zhao, Y. Tian, Y. Cui, X. Hao, Y. Yang, G. Qian, Dyes Pigm. 97 (1) (2013) 58–64.
[47] A. Warshel, M. Levitt, J. Mol. Biol. 103 (2) (1976) 227–249.
[48] J.T. Blair, K. Krogh jespersen, R.M. Levy, J. Am. Chem. Soc. 111 (18) (1989) 6948–6956.
[49] M.J. Paterson, J. Kongsted, O. Christiansen, K.V. Mikkelsen, C.B. Nielsen, J. Chem. Phys. 125 (18) (2006) 184501.
[50] H. Lin, D.G. Truhlar, Theor. Chem. Acc. 117 (2) (2007) 185–199.
[51] S. Canuto (Ed.), Combining Quantum Mechanics and Molecular Mechanics Some Recent Progresses in QM/MM Methods, Academic Press, San Diego, 2010.
[52] D.L. Silva, K. Coutinho, S. Canuto, Mol. Phys. 108 (21–23) (2010) 3125–3130.
[53] K. Coutinho, S. Canuto, M.C. Zerner, J. Chem. Phys. 112 (22) (2000) 9874–9880.
[54] K. Coutinho, S. Canuto, J. Chem. Phys. 113 (20) (2000) 9132–9139.
[55] S. Canuto (Ed.), Solvation Effects on Molecules and Biomolecules Computational Methods and Applications, Springer, New York, 2008.
[56] B.J. Orr, J.F. Ward, Mol. Phys. 20 (3) (1971) 513–526.
[57] M. Albota, D. Beljonne, J.L. Bredas, J.E. Ehrlich, J.Y. Fu, A.A. Heikal, S.E. Hess, T. Kogej, M.D. Levin, S.R. Marder, D. McCord-Maughon, J.W. Perry, H. Rockel, M. Rumi, C. Subramaniam, W.W. Webb, X.L. Wu, C. Xu, Science 281 (5383) (1998) 1653–1656.
[58] T. Kogej, D. Beljonne, F. Meyers, J.W. Perry, S.R. Marder, J.L. Bredas, Chem. Phys. Lett. 298 (1–3) (1998) 1–6.
[59] X.-J. Liu, J.-K. Feng, A.-M. Ren, X. Zhou, Chem. Phys. Lett. 373 (1–2) (2003) 197–206.
[60] X. Zhou, A.-M. Ren, J.-K. Feng, X.-J. Liu, Y.-D. Zhang, ChemPhysChem 4 (9) (2003) 991–997.
[61] Y. Zhao, A.-M. Ren, J.-K. Feng, C.-C. Sun, J. Chem. Phys. 129 (1) (2008) 014301.
[62] R. Zalesny, W. Bartkowiak, S. Styrcz, J. Leszczynski, J. Phys. Chem. A 106 (16) (2002) 4032–4037.
[63] N.A. Murugan, J. Kongsted, Z. Rinkevicius, K. Aidas, K.V. Mikkelsen, H. Agren, Phys. Chem. Chem. Phys. 13 (27) (2011) 12506–12516.
[64] D.L. Silva, N.A. Murugan, J. Kongsted, Z. Rinkevicius, S. Canuto, H. Agren, J. Phys. Chem. B 116 (28) (2012) 8169–8181.
[65] S. Mukamel, J. Chem. Phys. 77 (1) (1982) 173–181.
[66] J.P. Bergsma, P.H. Berens, K.R. Wilson, D.R. Fredkin, E.J. Heller, J. Phys. Chem. 88 (3) (1984) 612–619.
[67] M. Barbatti, A.J.A. Aquino, H. Lischka, Phys. Chem. Chem. Phys. 12 (19) (2010) 4959–4967.
[68] J.W. Ponder, F.M. Richards, J. Comput. Chem. 8 (7) (1987) 1016–1024.
[69] L. Verlet, Phys. Rev. 159 (1) (1967) 98–103.
[70] W.C. Swope, H.C. Andersen, P.H. Berens, K.R. Wilson, J. Chem. Phys. 76 (1) (1982) 637–649.
[71] H.J.C. Berendsen, J.P.M. Postma, W.F. Vangunsteren, A. Dinola, J.R. Haak, J. Chem. Phys. 81 (8) (1984) 3684–3690.
[72] U. Essmann, L. Perera, M.L. Berkowitz, T. Darden, H. Lee, L.G. Pedersen, J. Chem. Phys. 103 (19) (1995) 8577–8593.
[73] W.L. Jorgensen, J. Chandrasekhar, J.D. Madura, R.W. Impey, M.L. Klein, J. Chem. Phys. 79 (2) (1983) 926–935.
[74] W.L. Jorgensen, D.S. Maxwell, J. TiradoRives, J. Am. Chem. Soc. 118 (45) (1996) 11225–11236.
[75] H.J.C. Berendsen, J.P.M. Postma, W.F. van Gunsteren, J. Hermans, in: B. Pullman (Ed.), Intermolecular Forces, Reidel, Dordrecht, 1981, pp. 331–342.
[76] C.M. Breneman, K.B. Wiberg, J. Comput. Chem. 11 (3) (1990) 361–373.
[77] A.D. Becke, J. Chem. Phys. 98 (7) (1993) 5648–5652.
[78] C.T. Lee, W.T. Yang, R.G. Parr, Phys. Rev. B 37 (2) (1988) 785–789.
[79] M.J. Frisch, G.W. Trucks, H.B. Schlegel, G.E. Scuseria, M.A. Robb, J.R. Cheeseman, J.J.A. Montgomery, T. Vreven, K.N. Kudin, J.C. Burant, J.M. Millam, S.S. Iyengar, J. Tomasi, V. Barone, B. Mennucci, M. Cossi, G. Scalmani, N. Rega, G.A. Petersson, H. Nakatsuji, M. Hada, M. Ehara, K. Toyota, R. Fukuda, J. Hasegawa, M. Ishida, T. Nakajima, Y. Honda, O. Kitao, H. Nakai, M. Klene, X. Li, J.E. Knox, H.P. Hratchian, J.B. Cross, C. Adamo, J. Jaramillo, R. Gomperts, R.E. Stratmann, O. Yazyev, A.J. Austin, R. Cammi, C. Pomelli, J.W. Ochterski, P.Y. Ayala, K. Morokuma, G.A. Voth, P. Salvador, J.J. Dannenberg, V.G. Zakrzewski, S. Dapprich, A.D. Daniels, M.C. Strain, O. Farkas, D.K. Malick, A.D. Rabuck, K. Raghavachari, J.B. Foresman, J.V. Ortiz, Q. Cui, A.G. Baboul, S. Clifford, J. Cioslowski, B.B. Stefanov, G. Liu, A. Liashenko, P. Piskorz, I. Komaromi, R.L. Martin, D.J. Fox, T. Keith, M.A. Al-Laham, C.Y. Peng, A. Nanayakkara, M. Challacombe, P.M.W. Gill, B. Johnson, W. Chen, M.W. Wong, C. Gonzalez, J.A. Pople, Gaussian 03, Revision D.01, Gaussian, Inc., Wallingford, CT, 2004.
[80] D.P. Craig, T. Thirunamachandran, Molecular Quantum Electrodynamics – An Introduction to Radiation Molecule Interation, Dover Publications, New York, 1998.
[81] P.R. Monson, W.M. McClain, J. Chem. Phys. 53 (1) (1970) 29–37.
[82] W.M. McClain, J. Chem. Phys. 55 (6) (1971) 2789–2796.
[83] G.L.C. Moura, A.M. Simas, J. Phys. Chem. C 114 (13) (2010) 6106–6116.
[84] K. Ohta, K. Kamada, J. Chem. Phys. 124 (12) (2006) 124303.
[85] K. Ohta, L. Antonov, S. Yamada, K. Kamada, J. Chem. Phys. 127 (8) (2007) 084504.
[86] M.C. Zerner, ZINDO, A Semi-empirical Program Package, University of Florida, Gainsesville, FL 32611, 2000.
[87] W.A. Parkinson, M.C. Zerner, J. Chem. Phys. 90 (10) (1989) 5606–5611.
[88] N. Mataga, K. Nishimoto, Z. Physik, Z. Physik. Chem. 13 (3–4) (1957) 140–157.

[89] R.C. Barreto, D.L. Silva, PHOTON2: A Program to Calculate the Second Order Hyperpolarizability Using the Sum-Over-States (SOS) Method, 1.0, University of São Paulo, Brazil, 2012.
[90] R. Bauernschmitt, R. Ahlrichs, Chem. Phys. Lett. 256 (4–5) (1996) 454–464.
[91] R.E. Stratmann, G.E. Scuseria, M.J. Frisch, J. Chem. Phys. 109 (19) (1998) 8218–8224.
[92] M.E. Casida, C. Jamorski, K.C. Casida, D.R. Salahub, J. Chem. Phys. 108 (11) (1998) 4439–4449.
[93] S. Canuto, K. Coutinho, D. Trzesniak, in: J.R. Sabin, E. Brändas (Eds.), Advances in Quantum Chemistry, Academic Press, San Diego, 2002, pp. 161–183.
[94] H.C. Georg, K. Coutinho, S. Canuto, J. Chem. Phys. 126 (3) (2007) 034507.
[95] V.A. Shakin, S. Abe, T. Kobayashi, Phys. Rev. B 53 (16) (1996) 10656–10666.